# Numerical aspects of finite elastoplasticity with isotropic ductile damage for metal forming

**Khémais Saanouni — Abdelhakim Cherouat — Youssef Hammi**

*Université de Technologie de Troyes, GSM/LASMIS*
*12, rue Marie Curie BP 2060*
*F-10010 Troyes Cedex*

ABSTRACT. *This work is devoted to the study of an efficient numerical algorithm for evaluating damaged-plastic response of a material submitted to large plastic deformations. Fully coupled constitutive equations accounting for both combined isotropic and kinematic hardening as well as the ductile damage are formulated in the framework of Continuum Damage Mechanics (CDM). The associated numerical aspects concerning both the local integration of the coupled constitutive equations and the (global) equilibrium integration schemes are presented and implemented into a general purpose Finite Element code (ABAQUS). For the local integration of the fully coupled constitutive equations an efficient implicit and asymptotic scheme is used. Special care is given to the consistent tangent stiffness matrix derivation as well as to the reduction of the number of constitutive equations. Some numerical results are presented to show the numerical performance of the proposed stress calculation algorithm and the capability of the approach to predict the damage initiation and growth during a given metal forming process.*

RÉSUMÉ. *Ce travail est dévolu à l'étude d'un schéma incrémental pour l'évaluation de la réponse plastique-endommagée d'un matériau soumis à des incréments de déplacement en transformations finies. Des équations de comportement élastoplastique avec écrouissage mixte et endommagement ductile sont présentées dans le cadre de la thermodynamique des processus irréversibles avec variables d'état incluant l'endommagement continu. Les aspects numériques concernant l'intégration locale des équations constitutives ainsi que le schéma global de résolution du problème d'équilibre avec implémentation dans la plate-forme ABAQUS sont discutés. Pour l'intégration locale du modèle couplé un schéma asymptotique implicite est utilisé. Une attention particulière est accordée au calcul de la matrice tangente consistante et à la réduction du nombre des équations à résoudre. Quelques résultats numériques sont présentés pour montrer les performances numériques du schéma de calcul des contraintes proposé et pour illustrer la capacité de la modélisation à prédire l'amorçage et la croissance de l'endommagement ductile dans un procédé de mise en forme.*

KEYWORDS: *Finite elastoplasticity, ductile damage, stress computation, consistent tangent operator, finite elements, numerical simulation, metal forming.*

MOTS-CLÉS : *élastoplasticité, endommagement ductile, grandes déformations, calcul des contraintes, operateur tangent, éléments finis, simulation numérique, mise en forme.*

## 1. Introduction

Displacement-based finite element codes that are industrially utilized for the static or dynamic analysis of mechanical structures require accurate and efficient constitutive equations subroutines. This accuracy concerns both the description of the physical phenomena taken into account by those constitutive equations, as well as their numerical discretization with respect to time and space. This leads, in general, to highly non linear algebraic systems to be solved on both local and global levels.

For the global level, the spatial discretization of the principle of virtual work (or power) leads to a non-linear system for displacement (or velocity) field under the form of partial differential equations (PDE). This algebraic system is usually linearized to be solved for each load increment by either an implicit iterative Newton-type strategy, or a dynamic explicit or implicit one. Through linearization, many terms arise which can be classified into two classes : the first contains the material non linearity related to the material behavior (stress, internal variables) or the friction behavior; and the second contains the geometrical non linearities related to the finite deformations and rotations as well the evolving contact conditions. Particularly, the derivative of the stress tensor with respect to the total deformation tensor is needed. Generally, this "incremental" stress differential differs from the "continuous" differential given directly by the constitutive equations of rate type. It has been shown (see [NAG 82], [SIM 85]) that the use of the incremental stress differential consistent with the time discretization scheme of the stress tensor leads to quadratic convergence. For the explicit strategy to solve the system of PDE, only the stress increment at each time step is needed.

The calculation of the stress increment at each time step needs the local integration of the overall constitutive equations representing the coupled physical phenomena. There exist various explicit or implicit integration schemes for ordinary differential equations (ODE). Experience has shown that implicit time integration schemes have the advantage of stability and are suitable for application to those constitutive equation involving yield and loading-unloading conditions. These conditions are generally modeled by constructing a special procedure as the elastic predictor and plastic corrector scheme.

When a metallic material is formed by large straining processes as forging, stamping, hydroforming and deep drawing, it experiences large irreversible deformations, leading to the formation of high strain localization zones caused by the nucleation and growth of micro defects (voids) generally referred to as ductile isotropic damage. Accordingly, to increase the efficiency and the predictive capabilities of the virtual forming tools, an accurate theoretical and numerical modeling of the damage initiation and growth under finite transformations should be taken into account. This can be achieved by using the coupled approach in the sense that the damage evolution equation is directly incorporated and fully coupled with the elastoplastic constitutive equations. This kind of approach has been employed by many authors using damage models based either on Gurson's theory ([GEL 85], [ARA 86], [ONA 88], [BON 91], [BRU 96], among many others), or on Continuum Damage Mechanics (CDM) in the Kachanov's sense ([MAT 87], [ZHU 92], [SAA 99], [HAM 00], [SAA 00]...). These fully coupled approaches allow the prediction of not only the large transformation of the processed workpiece as large deformations, rotations, and evolving boundary conditions, but also they can indicate where and when the damaged zones can appear inside the formed part during the process ([SAA 99], [HAM 00], [SAA 00]).

In the present work, fully coupled constitutive equations accounting for both combined isotropic and kinematic hardening as well as the ductile damage in the CDM framework are presented. The particular case of the fully isotropic and isothermal flow considering small elastic strains, large plastic strains, isotropic and kinematic hardening, isotropic damage and the evolving contact with friction is implemented into ABAQUS/STD. The associated numerical aspects concerning both the local integration of the coupled constitutive equations as well as the (global) equilibrium integration schemes are presented. For fully implicit resolution strategy, special care is given to the consistent stiffness matrix calculation. The integration of the coupled constitutive equations is realized thanks to the backward Euler scheme together with the asymptotic integration procedure pioneered by Freed and Walker [FRE 86]. The efficiency of this integration procedure in the 3D isotropic case, is enhanced by reducing the number of the constitutive equations from 14 to 2 as proposed by Simo and Taylor [SIM 85] and widely used since that (see [HAR 93], [DOG 93], [CHA 96], [HAM 00] among many others). The numerical implementation of the damage is made in such a manner that calculations can be executed with or without damage effect, *i.e.* coupled or uncoupled calculations.

## 2. Kinematical background

The transformation gradient $\underline{F}$ between the initial (undeformed and undamaged) and the current (deformed and damaged) configuration is multiplicatively decomposed so that the following classical definitions are used:

$$\underline{F} = \underline{F}^e \cdot \underline{F}^p \quad \text{and} \quad \underline{B} = \underline{F} \cdot \underline{F}^T \qquad [1]$$

$$\underline{L} = \dot{\underline{F}} \cdot \underline{F}^{-1} = \underline{D} + \underline{W} \qquad [2]$$

$$\underline{D} = \frac{1}{2}(\underline{L} + \underline{L}^T) \quad \text{and} \quad \underline{W} = \frac{1}{2}(\underline{L} - \underline{L}^T) \qquad [3]$$

where $\underline{B}$ is the total Eulerian left Cauchy-Green deformation tensor associated with the Cauchy stress tensor $\underline{\sigma}$; $\underline{L}$ is the spatial velocity gradient in the current configuration, $\underline{D}$ and $\underline{W}$ are respectively the pure strain rate and the material spin tensors. The superimposed dot $(\dot{\ })$ denotes the usual time derivative.

To satisfy the objectivity requirement, the so-called Rotated Frame Formulation (RFF) is used. This leads to express the constitutive equations in a rotated configuration obtained from the current one by an orthogonal rotation tensor $\underline{Q}$ defined by [DOG 89]:

$$\underline{Q}^T \cdot \dot{\underline{Q}} = \underline{W}_Q \qquad \text{with } \underline{Q}(t=0) = \underline{I} \tag{4}$$

Accordingly, for any symmetric second order tensor $\underline{T}$, the objective rotational derivative with respect to the rotating frame is given by:

$$\frac{D_Q \underline{T}}{D_Q t} = \dot{\underline{T}} + \underline{T} \cdot \underline{W}_Q - \underline{W}_Q \cdot \underline{T} \tag{5}$$

from which the classical Jaumann and Green-Nagdhi rotational derivatives can be easily obtained. On the other hand the objective rotated tensor $\underline{T}_Q$ by the rotation $\underline{Q}$ is given by:

$$\underline{T}_Q = \underline{Q}^T \cdot \underline{T} \cdot \underline{Q} \tag{6}$$

Its time and rotational derivatives are related by:

$$\dot{\underline{T}}_Q = \underline{Q}^T \cdot \frac{D_Q \underline{T}}{D_Q t} \cdot \underline{Q} \tag{7}$$

Consequently, the constitutive equations are formulated in the same way as under small strain hypothesis and their generalization to the large strain case is simply achieved by replacing all the tensorial variables by their rotated corresponding quantities by using the Eq. [6].

The second main question posed by the finite transformation aspect is how the total strain rate can be decomposed into elastic (reversible) and plastic (irreversible) parts. For the metallic materials, dealing with large plastic strain but small elastic strain, the total Eulerian strain rate tensor decomposition can be approximated by:

$$\underline{D} \approx \dot{\underline{\varepsilon}}_e^J + \underline{D}^p \tag{8}$$

where $\dot{\underline{\varepsilon}}_e^J$ is the Jaumann derivative (rotational objective derivative) of the elastic strain tensor (for simplicity the subscript J will be removed), and $\underline{D}^p$ is the plastic strain rate tensor defined by the constitutive equations as will be shown in the next section.

## 3. Coupled constitutive equations for metal forming

### 3.1. *State variables versus effective state variables*

The finite thermo-elastoplastic constitutive equations coupled with the continuous damage is developed in the framework of the classical thermodynamics of irreversible processes with state variables. For the sake of simplicity, this will be presented hereafter using the classical small strain notations keeping in mind that the generalization to the finite strain hypothesis is made according to the RFF formulation presented above. This formulation uses a unified yield surface for both plasticity and damage as in [SAA 94]. A more general formulation using two different (but coupled) yield surfaces can be found in [HAM 00].

Limiting ourselves to the simple first displacement gradient theory, two couples of external state variables are used, namely: (1) the total strain associated with the Cauchy stress tensors ($\underline{\varepsilon}$,$\underline{\sigma}$) and (2) the absolute temperature associated with the specific entropy (T,s). Five couples of internal variables are taken into account: (1) the (small) elastic strain representing the inelastic flow associated with the Cauchy stress tensor ($\underline{\varepsilon}^e$,$\underline{\sigma}$); (2) the normalized heat flux vector associated with the gradient of the absolute temperature ( $\vec{q}\,/T$, $\vec{g} = \text{grad}(T)$ ); (3) the isotropic hardening variables (r, R) representing the size of the yield surface in strain space (r) and stress space (R); (4) the tensorial (deviatoric) kinematic hardening variables ($\underline{\alpha}$, $\underline{X}$) representing the displacement of the center of the yield surface in strain space ($\underline{\alpha}$) and stress space ($\underline{X}$), (5) the isotropic damage variables (D, Y), in Chaboche's sense [CHA 78].

Suppose that the current configuration contains some isotropic ductile damage distribution *i.e.* a given homogeneous distribution of micro-defects such as voids and/or micro-cracks ; the concept of the effective stress ([CHA 78], [LEM 85]) together with the hypothesis of total energy equivalence [SAA 94] are used to define the effective state variables by:

$$\tilde{\underline{\sigma}} = \frac{\underline{\sigma}}{\sqrt{1-D}} \quad \text{and} \quad \tilde{\underline{\varepsilon}}^e = \sqrt{1-D}\,\underline{\varepsilon}^e \qquad [9]$$

$$\tilde{\underline{X}} = \frac{\underline{X}}{\sqrt{1-D}} \quad \text{and} \quad \tilde{\underline{\alpha}} = \sqrt{1-D}\,\underline{\alpha} \qquad [10]$$

$$\tilde{R} = \frac{R}{\sqrt{1-D}} \quad \text{and} \quad \tilde{r} = \sqrt{1-D}\,r \qquad [11]$$

where, for simplicity, it has been assumed that the damage effect on the elastic behavior is the same than on the hardening variables (both isotropic and kinematic).

These effective state variables are used in the state and dissipation potentials to derive the complete set of fully coupled constitutive equations for metal forming processes (see [CHA 78], [LEM 85], [LEM 92], [SAA 94] among others).

### 3.2. *State potential: state relations*

The Helmoltz free energy $\psi(\varepsilon_e, \underline{\alpha}, r, D, T)$ is taken as a state potential. It is supposed to be a convex function of all the deformation-like state variables defined above and additively decomposed into thermo-elastic/damage and plastic/damage contributions:

$$\rho\psi(\underline{\varepsilon}^e, \underline{\alpha}, r, D, T) = \rho\psi_{ted}(\underline{\tilde{\varepsilon}}^e, T) + \rho\psi_{pd}(\underline{\tilde{\alpha}}, \tilde{r}\ ; T) \qquad [12]$$

where $\rho$ is the material density in the current undamaged configuration and the variable T in the last term $\Psi_{pd}$ acts as a simple parameter. In this work, only isotropic phenomena are considered, and have the following state potential:

$$\rho\psi_{ted} = \frac{1}{2}\kappa(\underline{\tilde{\varepsilon}}^e : \underline{1})^2 + \mu(\underline{\tilde{\varepsilon}}^e : \underline{\tilde{\varepsilon}}^e) - (3\kappa + 2\mu)\alpha(T - T_0)(\underline{\tilde{\varepsilon}}^e : \underline{1}) - \frac{1}{2}\rho\frac{C_v}{T_0}(T - T_0)^2 \qquad [13]$$

$$\rho\psi_{pd} = \frac{1}{3}C\underline{\tilde{\alpha}} : \underline{\tilde{\alpha}} + \frac{1}{2}Q\tilde{r}^2 \qquad [14]$$

where $\kappa$ and $\mu$ are the classical Lame's constants of elasticity, $\alpha$ is the coefficient of thermal expansion, C is the kinematic hardening modulus, Q is the scalar isotropic hardening modulus, $T_0$ is the reference absolute temperature, $C_v$ is the classical specific heat parameter and $\underline{1}$ being the second order unit tensor.

By using the Clausius-Duhem Inequality (CDI) one can easily derive, after some algebraic manipulations, both the state relations (Eq. [15 to 19]) and the residual inequality (Eq. [20]) defining the volumetric dissipation:

– State relations:

$$\underline{\sigma} = \rho\frac{\partial\psi}{\partial\underline{\varepsilon}^e} = \tilde{\kappa}(\underline{\varepsilon}^e : \underline{1})\underline{1} + 2\tilde{\mu}\underline{\varepsilon}^e - (3\kappa + 2\mu)\tilde{\alpha}(T - T_0)\underline{1} \qquad [15]$$

$$s = -\frac{\partial\psi}{\partial T} = \frac{1}{\rho}(3\kappa + 2\mu)\tilde{\alpha}(\underline{\varepsilon}^e : \underline{1}) + \frac{C_v}{T_0}(T - T_0) \qquad [16]$$

$$\underline{X} = \rho\frac{\partial\psi}{\partial\underline{\alpha}} = \frac{2}{3}\tilde{C}\underline{\alpha} \qquad [17]$$

$$R = \rho\frac{\partial\psi}{\partial r} = \tilde{Q}r \qquad [18]$$

$$Y = -\rho\frac{\partial\psi}{\partial D} = Y_e + Y_k + Y_i \qquad [19]$$

$$Y_e = \frac{1}{2}\kappa(\underline{\varepsilon}^e : \underline{1})^2 + \mu(\underline{\varepsilon}^e : \underline{\varepsilon}^e) - \frac{1}{2}(3\kappa + 2\mu)\frac{\alpha}{\sqrt{1-D}}(T - T_0)(\underline{\varepsilon}^e : \underline{1}) \qquad [19a]$$

$$Y_k = \frac{1}{3}C\underline{\alpha} : \underline{\alpha} \qquad [19b]$$

$$Y_i = \frac{1}{2}Qr^2 \qquad [19c]$$

– Residual inequality:

$$\Phi = \underline{\sigma} : \underline{D}^p - \underline{X} : \underline{\dot{\alpha}} - R\dot{r} + Y\dot{D} - \vec{g}.\frac{\vec{q}}{T} \geq 0 \qquad [20]$$

Note that in the state relations above, the main material properties are affected by the damage according to:

– elasticity properties of damaged material: $\tilde{\kappa} = (1-D)\kappa$ and $\tilde{\mu} = (1-D)\mu$ [21]

– kinematic hardening modulus of damaged material: $\tilde{C} = (1-D)C$ [22]

– isotropic hardening modulus of damaged material: $\tilde{Q} = (1-D)Q$ [23]

– thermal expansion of the damaged material: $\tilde{\alpha} = \sqrt{1-D}\alpha$ [24]

### 3.3. *Dissipation potentials: complementary relations*

The volumetric total dissipation given above (Eq. [20]) should be identically verified for any selected dissipative phenomenon. In this equation the force-like variables namely: $\underline{\sigma}$, $\underline{X}$, R,Y are given by the state relations (Eq. [15 to 19]), and the flux variables should be defined by using the generalized standard materials [HAL 75]. This is achieved by introducing both yield functions and dissipation potentials for each class of dissipative phenomena. As a first approximation, the total dissipation is additively decomposed into two terms, namely: mechanical dissipation $\Phi^m$ (plasticity, hardening and damage) and thermal dissipation $\Phi^{th}$, each of them being supposed independently positive or zero:

$$\begin{aligned} \Phi^m &= \underline{\sigma} : \underline{D}^p - \underline{X} : \underline{\dot{\alpha}} - R\dot{r} + Y\dot{D} \geq 0 \\ \Phi^{th} &= -\vec{g}.\frac{\vec{q}}{T} \geq 0 \end{aligned} \qquad [25]$$

Each of these dissipations will be analyzed to derive the flux variables associated with each selected dissipative phenomenon.

### 3.3.1. *Thermal dissipation: fully coupled heat equation*

Classically, the heat equation is derived from Fourier's dissipation potential which is a quadratic scalar function of the force $g_i$. For thermoelastoplastic medium with mixed hardening and damage (strong coupling) the final form of the generalized heat equation can be written as follows [SAA 94]:

$$\begin{aligned} k\Delta T = -\underline{\sigma} : \underline{D}^p + \underline{X} : \underline{\dot{\alpha}} + R\dot{r} - \left( Y + (3\kappa + 2\mu)\frac{\alpha}{2\sqrt{1-D}} T(\underline{\varepsilon}^e : \underline{1}) \right)\dot{D} \\ + \left( \rho C_v \frac{T}{T_0} + (3\kappa + 2\mu)\sqrt{1-D}\,\alpha' T(\underline{\varepsilon}^e : \underline{1}) \right)\dot{T} \\ + \left( (3\kappa' + 2\mu')\tilde{\alpha}(\underline{\varepsilon}^e : \underline{1}) + (3\kappa + 2\mu)\tilde{\alpha} T(\underline{\dot{\varepsilon}}^e : \underline{1}) \right) T \end{aligned} \qquad [26]$$

where $\Delta(T)$ stands for the Laplacian of the temperature and the prime (X') indicates the derivative of X with respect to temperature. The weak form of the partial differential equation Eq. [26] can be discretized with respect to time (Finite Difference Method) and space (Finite Elements Method) and solved together with the discretized weak form of the equilibrium problem thanks to a sequential methods.

### 3.3.2. *Mechanical dissipation: fully coupled constitutive equations*

In the present case of time independent flow, a yield function in the stress space $f(\underline{\sigma}, \underline{X}, R; D, T)$ and a plastic potential (non associative theory [LEM 85]) $F(\underline{\sigma}, \underline{X}, R; D, T)$ are introduced to derive the constitutive equations for plasticity with damage effect:

$$f = \left\| \underline{\tilde{\sigma}} - \underline{\tilde{X}} \right\| - \tilde{R} - \sigma_y < 0 \qquad [27]$$

$$F = f + \frac{3}{4}\frac{a}{C}\underline{\tilde{X}} : \underline{\tilde{X}} + \frac{1}{2}\frac{b}{Q}\tilde{R}^2 + \frac{S}{s+1}\left[\frac{Y}{S}\right]^{s+1} \frac{1}{(1-D)^\beta} \qquad [28]$$

where the temperature dependent material constants a and b are the non linearity parameters for kinematic (a) and isotropic (b) hardening respectively; while S, s and $\beta$ characterize the ductile damage evolution and the parameter $\sigma_y$ represents the initial size of the plastic yield surface. The notation $\left\| \underline{\tilde{\sigma}} - \underline{\tilde{X}} \right\|$ defines the norm of the effective stress according to:

$$\left\|\underline{\sigma}-\underline{X}\right\|=\sqrt{\frac{3}{2}\left(\underline{\sigma}^{d}-\underline{X}\right):\left(\underline{\sigma}^{d}-\underline{X}\right)} \qquad [29]$$

where $\underline{\sigma}^{d}$ is the deviatoric part of the stress tensor.

The generalized normality rule allows the derivation of the complementary relations for plasticity, with hardening including the damage effect:

$$\underline{D}^{p}=\dot{\lambda}\frac{\partial F}{\partial \underline{\sigma}}=\dot{\lambda}\frac{\partial f}{\partial \underline{\sigma}}=\dot{\lambda}\underline{n} \qquad [30]$$

$$\dot{\underline{\alpha}}=-\dot{\lambda}\frac{\partial F}{\partial \underline{X}}=\underline{D}^{p}-a\dot{\lambda}\underline{\alpha} \qquad [31]$$

$$\dot{r}=-\dot{\lambda}\frac{\partial F}{\partial R}=\frac{\dot{\lambda}}{\sqrt{1-D}}\left(1-b\tilde{r}\right) \qquad [32]$$

$$\dot{D}=\dot{\lambda}\frac{\partial F}{\partial Y}=\dot{\lambda}\left[\frac{Y}{S}\right]^{s}\frac{1}{(1-D)^{\beta}}=\dot{\lambda}\hat{Y} \qquad [33]$$

The tensor $\underline{n}$ represents the outward normal to the yield surface in the stress space given by:

$$\underline{n}=\frac{\partial f}{\partial \underline{\sigma}}=\frac{\partial F}{\partial \underline{\sigma}}=\frac{3}{2}\frac{1}{\sqrt{1-D}}\frac{(\underline{\sigma}^{d}-\underline{X})}{\left\|\underline{\sigma}-\underline{X}\right\|} \qquad [34]$$

The accumulated plastic strain rate $\dot{p}$ can be calculated from Eq. [30] using the following norm:

$$\dot{p}=\sqrt{\frac{2}{3}\underline{D}^{p}:\underline{D}^{p}}=\frac{\dot{\lambda}}{\sqrt{1-D}} \qquad [35]$$

which indicates that the isotropic hardening strain r is not equal to the accumulated plastic strain p unless the hardening is linear (b = 0) as clearly indicated by the Eq. [32]. The plastic multiplier $\dot{\lambda}$ is given by the classical consistency condition applied to the yield function f: $f > 0$, $\dot{\lambda} > 0$, $\dot{\lambda} f = 0$. This gives for the fully isotropic flow:

$$3\mu\sqrt{1-D}\frac{\left(\underline{\sigma}^{d}-\underline{X}\right)}{\left\|\underline{\sigma}-\underline{X}\right\|}:\underline{D}+H_{T}\dot{T}-H_{H}\dot{\lambda}=0 \qquad [36]$$

giving

$$\dot{\lambda}=\frac{1}{H_{H}}\left\langle 3\mu\sqrt{1-D}\frac{\left(\underline{\sigma}^{d}-\underline{X}\right)}{\left\|\underline{\sigma}-\underline{X}\right\|}:\underline{D}+H_{T}\dot{T}\right\rangle \qquad [37]$$

where <(.)> stands for the positive part of (.) *and* $H_H > 0$ is the tangent plastic modulus given by :

$$H_H = 3\mu + Q + C + \frac{1}{2}\frac{\sigma_y}{1-D}\hat{Y} - \left[ b\tilde{R} + \frac{3}{2} a \frac{\left(\underline{\sigma}^d - \underline{X}\right)}{\left\|\underline{\sigma} - \underline{X}\right\|} : \underline{\tilde{X}} \right] \qquad [38]$$

and $H_T$ represents the thermal effect given by:

$$H_T = 3\left[ \mu' \frac{1+\nu}{E} \underline{\tilde{\sigma}} - \frac{1}{2}\frac{C'}{C} \underline{\tilde{X}} \right] : \frac{\left(\underline{\sigma}^d - \underline{X}\right)}{\left\|\underline{\sigma} - \underline{X}\right\|} - \frac{Q'}{Q}\tilde{R} - \sigma'_y \qquad [39a]$$

If the variation of the Poisson's ration $\nu$ with the temperature is neglected, the Eq. [39.a] writes under the following simpler form:

$$H_T = \frac{3}{2}\left[ \frac{E'}{E} \underline{\tilde{\sigma}} - \frac{C'}{C} \underline{\tilde{X}} \right] : \frac{\left(\underline{\sigma}^d - \underline{X}\right)}{\left\|\underline{\sigma} - \underline{X}\right\|} - \frac{Q'}{Q}\tilde{R} - \sigma'_y \qquad [39b]$$

Note that, in this unified formulation, a single yield function is taken for both plasticity and damage, leading to a single plastic multiplier. This restrictive choice is justified in the case of metal forming where the damage develops only on material points with large plastic deformation. However, for some other materials as concrete or composite structures, damage can develops without plasticity and vice versa. In that cases the use of multisurface formulation should be preferred : one yield function for plasticity with damage effect (coupling) and another one for the damage yielding [HAM 00].

Finally, the direct time derivative of the stress tensor (Eq. [15]) gives with the help of the Eq. [37]

$$\underline{\dot{\sigma}} = \underline{\underline{L}}^{epd} : \underline{D} + \underline{L}^{Ted}\dot{T} \qquad [40]$$

with:

$$\underline{\underline{L}}^{epd} = \begin{cases} \underline{\underline{\tilde{\Lambda}}} \text{ if } \dot{\lambda} = 0 \\ \underline{\underline{\tilde{\Lambda}}} - \frac{3\tilde{\mu}}{H_H}\left[ \frac{3\mu}{\left\|\underline{\sigma} - \underline{X}\right\|^2}\left(\underline{\sigma}^d - \underline{X}\right) \otimes \left(\underline{\sigma}^d - \underline{X}\right) + \frac{\hat{Y}}{1-D}\left(\underline{\sigma}^d - \underline{X}\right) \otimes \underline{\tilde{\sigma}} \right] \text{ if } \dot{\lambda} > 0 \end{cases} \qquad [41]$$

and:

$$\underline{L}^{Ted} = \begin{cases} \underline{L}_0^{Ted} \text{ if } \dot{\lambda} = 0 \\ \underline{L}_0^{Ted} - \sqrt{1-D}\,\frac{H_T}{H_H}\left[ 3\mu \frac{\left(\underline{\sigma}^d - \underline{X}\right)}{\left\|\underline{\sigma} - \underline{X}\right\|} + \frac{\hat{Y}}{1-D}\underline{\tilde{\sigma}} \right] \text{ if } \dot{\lambda} > 0 \end{cases} \qquad [42]$$

where use has been made of the following notations ( $\underset{=}{1}$ being the fourth order unit tensor):

$$\underset{\approx}{\tilde{\Lambda}} = (1-D)\underset{\approx}{\Lambda} = (1-D)\left[2\mu\underset{=}{1} + \kappa\underline{1}\otimes\underline{1}\right] = 2\tilde{\mu}\underset{=}{1} + \tilde{\kappa}\underline{1}\otimes\underline{1} \qquad [43]$$

is the classical fourth order symmetric operator of the isotropic elastic properties affected by the damage, and:

$$\underline{L}_0^{Ted} = \sqrt{1-D}\begin{bmatrix} 2\mu'\left[\underline{\tilde{\varepsilon}}^e - \alpha(T-T_0)\right] + \kappa'\left[\underline{\tilde{\varepsilon}}^e : \underline{1} - 3\alpha(T-T_0)\right]\underline{1} \\ + (3\kappa+2\mu)\left[\alpha'(T-T_0) - \alpha\right]\underline{1} \end{bmatrix} \qquad [44]$$

is the thermoelastic contribution in the tangent operator.

It is clear from the equations [40] and [41] that the continuous tangent elastoplastic-damage operator is non symmetric for the coupled problem *i.e.* if Y is non zero.

## 4. Numerical implementation

In metal forming, the large deformation and damage behavior experienced by metallic materials are described by nonlinear equilibrium, the above presented coupled thermo-elastoplastic-damage constitutive equations and the contact conditions with frictional constitutive equations. For the sake of simplicity, in this paper we limit ourselves to solving the equilibrium problem associated with elastoplastic-damaged solids without thermal effect nor the contact/friction conditions (see [HAM 00] for more details).

### 4.1. *Finite element formulation*

The velocity (displacement) based finite element formulation starts with the principle of virtual power (work) which states that, among all the kinematically admissible velocity (displacement) fields $\dot{\mathbf{u}}^*$ ($\mathbf{u}^*$), the solution of the equilibrium problem minimizes the functional G (weak form) given here in continuous form limited to the quasi-static case using the classical updated Lagrangian formulation:

$$G(\dot{\mathbf{u}}^*, \dot{\mathbf{u}}) = \frac{1}{2}\int_V \underline{\sigma} : \underline{D}^* dV - \int_V \mathbf{f}.\dot{\mathbf{u}}^* dV - \int_{\Gamma_F} \mathbf{F}.\dot{\mathbf{u}}^* dS \qquad [45]$$

where V is the volume of the current configuration, $\Gamma_F$ is the boundary of the solid where external forces **F** (including the contact forces) are prescribed, **f** represents the vector of volumetric applied forces, $\underline{D}^*$ is the virtual strain rate tensor and $\underline{\sigma}$ is the stress tensor given by the coupled constitutive equations discussed above.

By applying the minimization principle to the spatially discretized form of Eq. [45], one can obtain for the overall structure:

$$\{\Re\} = \{F_{int}\} - \{F_{ext}\} = \{0\} \tag{46}$$

where $\Re$ is called the equilibrium residual vector; $F_{int}$ and $F_{ext}$ are the internal and external force vectors written here using the natural coordinates as:

$$\{F_{int}\} = \int_{V0} [B]^T \{\sigma\} J_v dV_0 \tag{47}$$

$$\{F_{ext}\} = \int_{V0} [N]^T \{f_v\} J_v dV_0 + \int_{\Gamma_{F0}} [N]^T \{F\} J_s dS_0 \tag{48}$$

where $V_0$ and $\Gamma_{F0}$ are the volume and its boundary of the reference solid element, $J_v$ is the Jacobian determinant of the isotropic transformation between global and natural coordinates for the solid element, $J_s$ is the Jacobian determinant for the surface element, N is the matrix of interpolation functions and B is the matrix of strain (rate) interpolation. Note that the matrices B, N and the Jacobians, $J_v$ and $J_s$ are functions of the displacements (geometrical non linearities).

The most widely used implicit iterative method to solve the system [46] is the Newton-Raphson method, which consists in linearizing Eq. [46], for the $(n+1)^{th}$ load increment and at the iteration (p+1), as follows :

$$\{\Re_{n+1}^{p+1}\} = \{\Re_{n+1}^{p}\} - \{K_{n+1}^{p}\}\left(\{U_{n+1}^{p+1}\} - \{U_{n+1}^{p}\}\right) + \ldots = \{0\} \tag{49}$$

where $\{U_{n+1}^{p}\}$ is the approximation of the solution at the iteration (p). The current tangent stiffness matrix $K_{n+1}^{p}$ is defined by:

$$\{K_{n+1}^{p}\} = \left.\frac{\partial \Re}{\partial U}\right|_{\{U_{n+1}^{p}\}} = \left.\left(\frac{\partial F_{int}}{\partial U} - \frac{\partial F_{ext}}{\partial U}\right)\right|_{\{U_{n+1}^{p}\}} = \{K_{n+1}^{p}\}^{int} - \{K_{n+1}^{p}\}^{ext} \tag{50}$$

The second term, $\{K_{n+1}^{p}\}^{ext}$ describes the dependence of the external loads on the geometry and will not be discussed herein. The first, $\{K_{n+1}^{p}\}^{int}$ represents the variation of the internal forces with displacements. As shown by Eq. [47], this variation is due to the stress $\underline{\sigma}$ (material non linearities) given by the fully coupled constitutive equations, and the fact that the matrix B as well as the Jacobien determinant $J_v$ are displacement dependent (geometrical non linearities). For the sake of simplicity, only the term related to the material non linearities will be discussed hereafter.

### 4.2. *Time integration procedure*

In order to calculate the internal forces $\{F^p_{n+1}\}^{int}$ and the tangent stiffness matrix $\{K^p_{n+1}\}^{int}$, we must first compute updated stresses at the end of the current load increment. This can be achieved by integrating the overall set of coupled constitutive equations discussed above. The implicit Euler integration scheme (Backward method) is used since it contains the property of absolute stability and the possibility of appending further equations to the existing system of nonlinear equations. Let us consider the system of ordinary differential equations given above (Eq. [30-35]) formally represented by $\dot{y} = f(y,t)$. The implicit method is defined by (for clarity the iteration subscript (p) is omitted):

$$y_{n+1} = y_n + f(y_{n+1}, t_n + \Delta t)\Delta t \tag{51}$$

with the abbreviations $y_{n+1} = y(t_n + \Delta t)$ and $y_n = y(t_n)$. When applied to the stress tensor for example, the Eq. [51] reads:

$$\sigma_{n+1} = \sigma_n + \dot{\sigma}(\sigma_{n+1}, X_{n+1}, R_{n+1}, D_{n+1})\Delta t \tag{52a}$$

Using the elasticity relation (Eq. [15]) and the decomposition of the strain tensor we get:

$$\underline{\sigma}_{n+1} = (1 - D_n - \dot{D}\Delta t)\underline{\underline{\Lambda}} : (\underline{\varepsilon}_n + \underline{\dot{\varepsilon}}\Delta t - \underline{\varepsilon}^p_n - \underline{\dot{\varepsilon}}^p \Delta t) \tag{52b}$$

where we have incorporated the fact that the plastic strain rate and damage rate only occur if the field condition is satisfied, *i.e.* during the time interval $\Delta t_p \leq \Delta t$. In the following, the subscript (n+1) will be omitted and the variables, which do not contain the subscript (n+1), are computed at $t_n + \Delta t$.

For the calculations of hardening variables $\underline{\alpha}$ and $r$; the AI 'Asymptotic Integration' procedure proposed by Freed and Walker [FRE 86], for a better integration of first-order ordinary equations is used. The AI procedure is mainly based on the fact that the above discussed constitutive equations have the following form:

$$\dot{Y} = \phi(Y)[A(Y) - Y] \tag{53}$$

Where Y denotes here a set of state variables to be considered and A(Y) and $\phi(Y)$ are given functions depending on the concerned constitutive equation. One can integrate Eq. [53] exactly over the time step and obtain the following recursive integral equation:

$$Y_{t+\Delta t} = \exp\left[-\int_t^{t+\Delta t}\phi(Y(\xi))d\xi\right] + \int_t^{t+\Delta t}\left[\exp\left[\int_t^{t+\Delta t}\phi(Y(\xi))d\xi\right]\phi(Y(\xi))A(Y(\xi))\right]d\xi \quad [54]$$

where $\xi$ is the parameter of time integration. Freed and Walker [FRE 92] have considered several discretization schemes of this exact solution. We retain here, the asymptotic integration scheme at time $t + \Delta t$ :

$$Y_{t+\Delta t} = e^{-\phi(Y_{t+\Delta t})\Delta t}Y_t + \left[1 - e^{-\phi(Y_{t+\Delta t})\Delta t}\right]A(Y_{t+\Delta t}) \quad [55]$$

Applied to the kinematic and isotropic hardening evolution equations this gives:

$$\underline{\alpha} = \underline{\alpha}_n \exp(-a\Delta\lambda) + \frac{1}{a}\left[1 - \exp(-a\Delta\lambda)\right]\underline{n} \quad [56]$$

$$r = r_n \exp(-b\Delta\lambda) + \frac{1}{b\sqrt{1-D}}\left[1 - \exp(-b\Delta\lambda)\right] \quad [57]$$

where $\Delta\lambda = \dot{\lambda}\Delta t$ is related to the accumulated plastic strain increment according to the Eq. [35].

By using the complete set of constitutive equations we end up with a system of 14 nonlinear scalar equations for 15 unknowns : six stresses, six back-stresses for kinematic hardening, one isotropic hardening stress, one isotropic damage variable and the plastic multiplier. The 14 first equations are:

$$\underline{\sigma}^d = (1-D)\underline{\sigma}_n^{\bullet} - 2\mu\sqrt{1-D}\Delta\lambda\underline{n} \quad [58]$$

$$\underline{X} = (1-D)\underline{X}_n\exp(-a\Delta\lambda) + \frac{2C}{3a}(1 - \exp(-a\Delta\lambda))\sqrt{1-D}\underline{n} \quad [59]$$

$$R = (1-D)QR_n \exp(-b\Delta\lambda) + \frac{Q}{b}(1 - \exp(-b\Delta\lambda))\sqrt{1-D} \quad [60]$$

$$D = D_n + \left[\frac{Y}{S}\right]^s \frac{\Delta\lambda}{(1-D)^\beta} \quad [61]$$

where: $$\underline{\sigma}_n^{\bullet} = 2\mu(\underline{\varepsilon}_n - \underline{\varepsilon}_n^p)^d = 2\mu(\underline{\varepsilon}^{\bullet})^d \quad [62]$$

The remaining (15$^{th}$) equation is given by the yield condition Eq. [27], which must be satisfied at the end of each time step.

Before solving iteratively (Newton's method) the above system of 15 equations, it is very helpful to reduce the size of this system by eliminating some equations among them. Following an idea originally proposed by Simo and Taylor [SIM 85] and widely used since that, we derive from Eq. [58] and [59] the deviatoric tensorial quantity $\underline{\sigma}^d$-$\underline{X}$ between t and t+$\Delta$t:

$$\underline{\sigma}^{d} - \underline{X} = (1-D)\underline{Z}_{n} - \sqrt{1-D}\left[2\mu\Delta\lambda + \frac{2C}{3a}(1-\exp(-a\Delta\lambda))\right]\underline{n} \qquad [63]$$

where the deviatoric tensor $\underline{Z}$ at $t_n$ is given by :

$$\underline{Z}_{n} = \underline{\sigma}_{n}^{*} - \frac{2}{3}C\underline{\alpha}_{n}\exp(-a\Delta\lambda) \qquad [64]$$

The multiplication of the yield function (Eq. [27]) by $\underline{\sigma}^{d}$-$\underline{X}$ gives

$$\underline{\sigma}^{d} - \underline{X} = \frac{2}{3}\left[R + \sqrt{1-D}\sigma_{y}\right]\underline{n} \qquad [65]$$

This implies:

$$\underline{Z} = \|\underline{Z}\|\underline{n} \qquad [66]$$

with the notation

$$\|\underline{Z}\| = \frac{1}{(1-D)}\left(R + \sqrt{1-D}\sigma_{y}\right) + \frac{1}{\sqrt{1-D}}\left[3\mu\Delta\lambda + \frac{C}{a}(1-\exp(-a\Delta\lambda))\right] \qquad [67]$$

Hence, the unknown tensor $\underline{n}$ is replaced by the tensor $\underline{Z}$, which depends only on one scalar unknown, namely $\Delta\lambda$ as shown by the Eq. [67].

Furthermore, the system of 15 equations is now restricted to two scalar equations, namely:

$$\begin{aligned} G_{1}(\Delta\lambda, D) = \|\underline{Z}\| - \frac{1}{(1-D)}\left(R + \sqrt{1-D}\sigma_{y}\right) & \\ - \frac{1}{\sqrt{1-D}}\left[3\mu\Delta\lambda + \frac{C}{a}(1-\exp(-a\Delta\Delta))\right] = 0 & \end{aligned} \qquad [68]$$

$$G_{2}(\Delta\lambda, D) = D - D^{n} - \left[\frac{Y}{S}\right]^{s}\frac{\Delta\lambda}{(1-D)^{\beta}} = 0 \qquad [69]$$

where the expression of the damage release rate Y (scalar) is given by :

$$\begin{aligned} Y = 2\mu\left(\underline{\varepsilon}^{*} : \underline{\varepsilon}^{*} + \frac{3(\Delta\lambda)^{2}}{2(1-D)} - \Delta\lambda\underline{n} : \underline{\varepsilon}^{*}\right) + \frac{C}{3}\left[\underline{\alpha}_{n}\exp(-a\Delta\lambda) + \frac{1}{a}(1-\exp(-a\Delta\lambda))\underline{n}\right]^{2} & \\ + \frac{Q}{2}\left[r_{n}\exp(-b\Delta\lambda) + \frac{1}{b\sqrt{1-D}}(1-\exp(-b\Delta\lambda))\right]^{2} & \end{aligned} \qquad [70]$$

This small system (Eq. [68-69]) is solved iteratively thanks to the Newton-

Raphson numerical integration procedure to compute the two unknowns : $\Delta\lambda$ and D (see [HAM 00] for details). Tables (1) and (2) summarize schematically the proposed stress calculation.

REMARK–. For plane stress hypothesis the total strain component $\varepsilon_{33}$ is not defined by the kinematics but by a new constraint namely : $G_3(\Delta\lambda, D, \varepsilon_{33}) = \sigma_{33} = 0$. This leads to an additional scalar equation with the new unknown $\varepsilon_{33}$ to be determined together with $\Delta\lambda$ and D by solving the three equations $G_1$, $G_2$ and $G_3$ [HAM 00].

### 4.3. *Consistent Elastoplastic-damage tangent operator*

As discussed in paragraph 4.1 the quasi-static tangent stiffness matrix for large deformation, is viewed as relating the rate of internal nodal forces to the nodal velocities. This gives rise to three main contributions: the stress contribution, the contact/friction contribution and geometry variation contribution. Only the first contribution is discussed here (see [HAM 00] for more details). The computation of this term needs the calculation of the tangent operator representing the stress variation with respect to the total strain for each load increment. The continuous form of this operator is given by Eq. [40] including thermal contribution. As reported by many authors, the equality of the global/local convergence of a Newton-Rahpson method is greatly improved when using a tangent stiffness matrix consistent with the discretized incrementation of the local constitutive equations ([NAG 82], [SIM 85]). This consistent operator is given here (thermal contribution being neglected) by differentiating with respect to the total strain, the time discretized expression of the stress as follows:

$$\underline{\underline{K}}^{epd}_{cons} = \frac{d\underline{\sigma}}{d\underline{\varepsilon}} = \frac{d}{d\underline{\varepsilon}}\left[(1-D)\kappa(\underline{\varepsilon}:\underline{1}) + (1-D)\underline{\sigma}^{*} - 2\mu(1-D)\Delta\lambda\underline{n}\right] \qquad [71]$$

This needs the calculation of the derivatives of D and $\Delta\lambda$ with respect to the total strain $\underline{\varepsilon}$. These are obtained by solving equations [68-69] and the final expression of the consistent tangent operator is [HAM 00]:

$$\frac{d\underline{\sigma}}{d\underline{\varepsilon}} = \underline{\underline{\tilde{\Lambda}}} - 2\mu(1-D)\left(\underline{n}\otimes\frac{d\lambda}{d\underline{\varepsilon}} + \Delta\lambda\frac{d\underline{\underline{n}}}{d\underline{\varepsilon}}\right) - \left(\kappa(\underline{\varepsilon}:\underline{1})\underline{1} + \underline{\sigma}^{*} - 2\mu\Delta\lambda\underline{n}\right)\otimes\frac{dD}{d\underline{\varepsilon}} \qquad [72]$$

The above discussed constitutive equations and the corresponding local time integration have been implemented in the general-purpose finite element code ABAQUS/STD thanks to the user's material subroutines UMAT for static implicit solving procedure.

| | |
|---|---|
| (I) | Calculate elastic predictor : |
| | $\underline{\sigma}^{\text{trial}} = (1 - D_n)\kappa(\underline{\varepsilon} : \underline{1})\underline{1} + 2\mu(1 - D_n)(\underline{\varepsilon} - \underline{\varepsilon}_n^p)^d$ |
| | If $F < 0$ set $\underline{\sigma} = \underline{\sigma}^{\text{trial}}$, $\underline{X} = \underline{X}_n$, $R = R_n$, $D = D_n$ and $\lambda = \lambda_n$ |
| | Else if $F \geq 0$ continue with (II) otherwise EXIT |
| (II) | Calculate $(\Delta\lambda, D)$ and hence $\underline{n} = \underline{Z}/\lVert\underline{Z}\rVert$, according to Table 2. |
| (III) | Calculate stresses with plastic corrector : |
| | $\underline{\sigma}^d = (1 - D_n)\underline{\sigma}^* - 2\mu(1 - D)\Delta\lambda\underline{n}$ and $\underline{\sigma} = (1 - D)\kappa(\underline{\varepsilon} : \underline{1})\underline{1} + \underline{\sigma}^d$ |
| (IV) | Calculate the hardening stresses :$\underline{\alpha}$ Eq. [56] and r Eq.[57] |

**Table 1.** *Computation of the Cauchy and internal stresses*

$$\underline{Z}^{(p)} = \underline{\sigma}^* - \frac{2}{3}C\alpha_n \exp\left(-a\Delta\Delta^{(p)}\right)$$

$$G_1^{(p)}\left(\Delta\lambda^{(p)}, D^{(p)}\right) = \text{Eq. [68]}$$

$$G_2^{(p)}\left(\Delta\lambda^{(p)}, D^{(p)}\right) = \text{Eq. [69]}$$

$$G_{1\lambda}^{'(p)} = \frac{\partial G_1^{(p)}}{\partial \lambda}, \quad G_{1D}^{'(p)} = \frac{\partial G_1^{(p)}}{\partial D}, \quad G_{2D}^{'(p)} = \frac{\partial G_2^{(p)}}{\partial D}, \quad G_{2\lambda}^{'(p)} = \frac{\partial G_2^{(p)}}{\partial \lambda}$$

$$\delta D = \left(G_2^{(p)}G_{1\lambda}^{'(p)} - G_1^{(p)}G_{2\lambda}^{'(p)}\right)\left(G_{1D}^{'(p)}G_{2\lambda}^{'(p)} - G_{1\lambda}^{'(p)}G_{2D}^{'(p)}\right)^{-1}$$

$$\delta\lambda = -\left(G_{1\lambda}^{'(p)}\right)^{-1}\left(G_1^{(p)} - G_{1D}^{'(p)}\delta D\right)$$

$$\Delta\lambda^{(p+1)} = \lambda^{(p)} + \delta\lambda \quad \text{and} \quad D^{(p+1)} = D^{(p)} + \delta D$$

$$\text{if} \begin{cases} \left|G_1^{(p+1)}\left(\Delta\lambda^{(p+1)}, D^{(p+1)}\right)\right| \leq \varepsilon_1 \\ \left|G_2^{(p+1)}\left(\Delta\lambda^{(p+1)}, D^{(p+1)}\right)\right| \leq \varepsilon_2 \end{cases} \text{EXIT}$$

Otherwise start form the beginning

**Table 2.** *Computation of $\Delta\lambda$ and D by Newton-Raphson method ((p) stands for iterations)*

## 5. Numerical examples

### 5.1. *Accuracy contemplation*

Let's now investigate some effects of both hardening and damage on the numerical accuracy of the proposed stress algorithm. The convergence properties of the algorithm will be studied on a large domain, covering ranges of relative errors between 1 and $10^{-7}$. The selected loading conditions are a two-steps loading path under strain control:

– first step: uniaxial strain path with $\varepsilon_{11} = 5\%$ $\varepsilon_{12} = 0$

– the second step: multiaxial strain path with $\varepsilon_{11} = 5\%$ $\varepsilon_{12} = 5\%$

– This defines a non-proportional tensile-shear loading path making an angle of 90° between the actual normal to the yield surface and the stress increment.

The relative error measure is defined by

$$\text{Error} = \frac{\|y_n - y_{ref}\|}{\|y_{ref}\|} \qquad \text{for} \qquad n = 10, 100, 1\,000, 10\,000$$

where n is the number of increments and $y_{ref}$ is the reference solution calculated with n = 100 000 load increments. These increments are constant for each path and equally distributed on the two loading steps. The Newton iterations are stopped for a maximum relative error of $10^{-10}$.

Figures 1 and 2 summarize the obtained results. First the equivalent stress error is plotted versus the equivalent (cumulated) plastic strain error (Figure 1) where it is clear that the error is less than 0.001 for n= 1 000 increments. Figure 2 shows the damage error versus the equivalent plastic strain error which is still lower than 0.001 for the same number of iterations. From this figure it's clear that the convergence rate is linear and better for accumulated plastic strain than for damage.

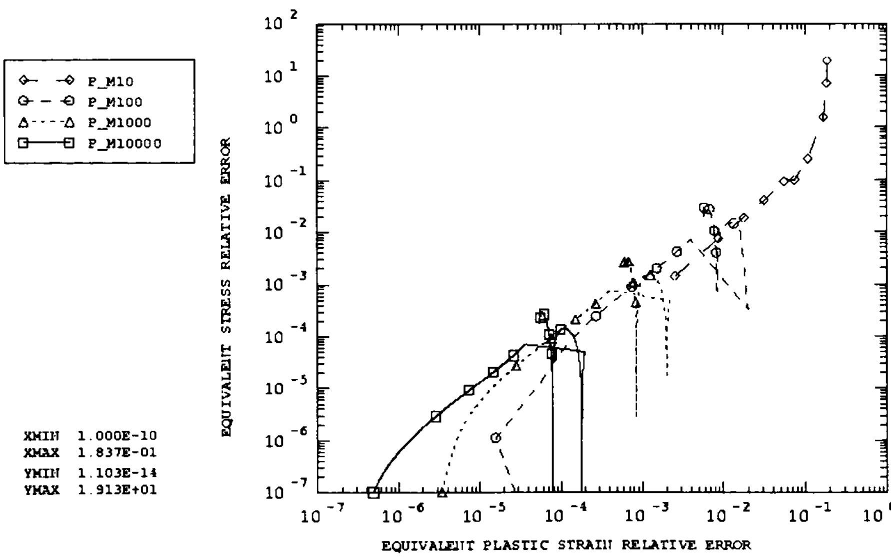


**Figure 1.** *Equivalent stress versus cumulated plastic strain relative errors*

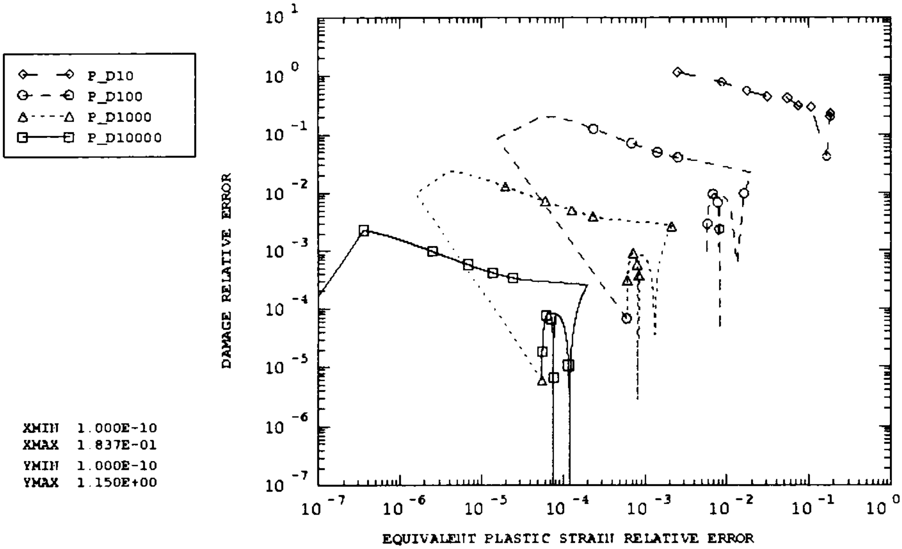


**Figure 2.** *Damage versus cumulated plastic strain relative errors*

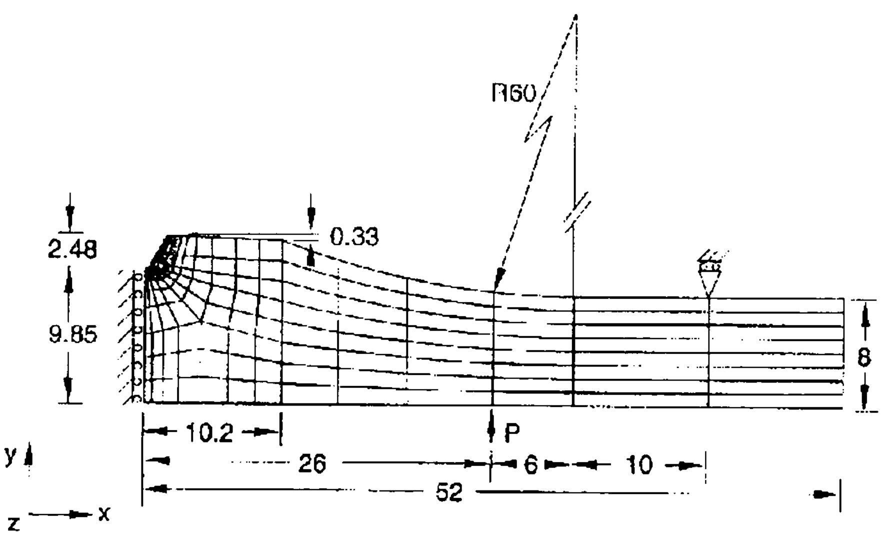


**Figure 3.** *Modeling of the quarter of the plane strain notched bar [DOG 93]*

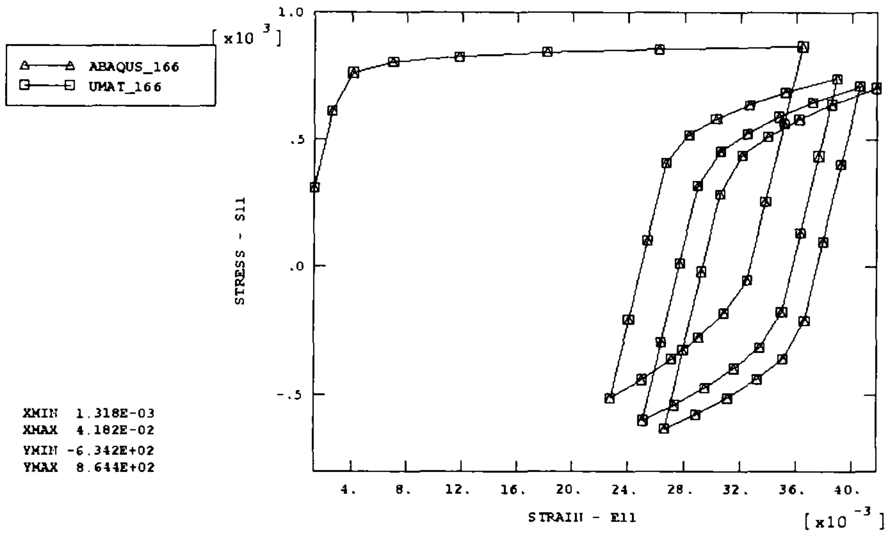


**Figure 4.** *Stress-strain response in the vicinity of the notch root during the first 4 loading cycles*

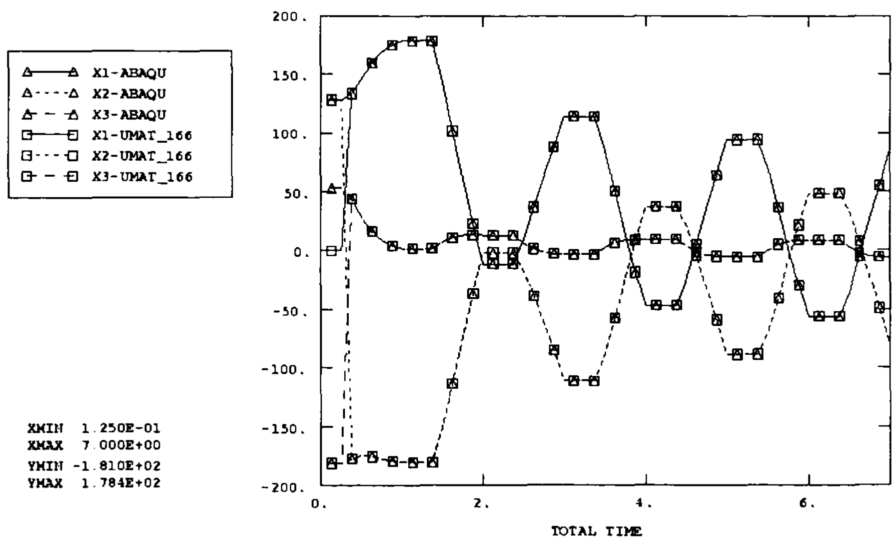


**Figure 5.** *Evolution of the back stress tensor components during the first 4 loading cycles*

### 5.2. *Notched bar under bending cyclic strain conditions*

The selected example is a notched bar subjected to a cyclic 4-points bending load, assuming plane strain state condition, already investigated by Doghri [DOG 93]. The calculation is achieved using the same mesh used by Doghri with the material parameters E = 210.0 GPa, $\nu$ = 0.3, $\sigma_y$ = 200.0 MPa, Q = 520.0 MPa, b = 0.26, C = 25 500.0 MPa, a = 81.0, and the boundary conditions shown in Figure 3.

| **Number of iterations** | | | | **Number of iterations** | | | |
|---|---|---|---|---|---|---|---|
| Nb load step | Increm. Number | Abaqus | Umat | Nb load step | Increm. Number | Abaqus | Umat |
| 1 | 1 | 1 | 1 | 2 | 21 | 1 | 1 |
| 1 | 2 | 3 | 3 | 2 | 22 | 1 | 1 |
| 1 | 3 | 3 | 3 | 2 | 23 | 2 | 2 |
| 1 | 4 | 3 | 3 | 2 | 24 | 2 | 2 |
| 1 | 5 | 2 | 2 | 2 | 25 | 2 | 2 |
| 1 | 6 | 3 | 3 | 2 | 26 | 1 | 1 |
| 1 | 7 | 3 | 3 | 2 | 27 | 1 | 1 |
| 1 | 8 | 3 | 3 | 2 | 28 | 2 | 2 |
| 2 | 1 | 2 | 3 | 2 | 29 | 2 | 2 |
| 2 | 2 | 1 | 1 | 2 | 30 | 2 | 2 |
| 2 | 3 | 1 | 1 | 2 | 31 | 2 | 2 |
| 2 | 4 | 1 | 1 | 2 | 32 | 3 | 3 |
| 2 | 5 | 1 | 1 | 2 | 33 | 3 | 3 |
| 2 | 6 | 1 | 1 | 2 | 34 | 1 | 1 |
| 2 | 7 | 1 | 1 | 2 | 35 | 1 | 1 |
| 2 | 8 | 2 | 2 | 2 | 36 | 1 | 1 |
| 2 | 9 | 2 | 2 | 2 | 37 | 2 | 2 |
| 2 | 10 | 1 | 1 | 2 | 38 | 2 | 2 |
| 2 | 11 | 1 | 1 | 2 | 39 | 2 | 2 |
| 2 | 12 | 2 | 2 | 2 | 40 | 2 | 2 |
| 2 | 13 | 2 | 2 | 2 | 41 | 2 | 2 |
| 2 | 14 | 2 | 2 | 2 | 42 | 1 | 1 |
| 2 | 15 | 2 | 2 | 2 | 43 | 1 | 1 |
| 2 | 16 | 3 | 3 | 2 | 44 | 2 | 2 |
| 2 | 17 | 5 | 5 | 2 | 45 | 2 | 2 |
| 2 | 18 | 1 | 1 | 2 | 46 | 2 | 2 |
| 2 | 19 | 1 | 1 | 2 | 47 | 2 | 2 |
| 2 | 20 | 1 | 1 | 2 | 48 | 3 | 3 |

**Table 3.** *Comparison of the iteration number for both ABAQUS and Umat for the calculation shown in Figures 4 & 5*

First we start with a comparison between our model (Umat) without damage and the standard nonlinear isotropic/kinematic hardening available in ABAQUS/STD. The Figure 4 shows that the local material response (of element 166 located at the notch root) in term of the first component of the Cauchy stress versus the first component of plastic strain obtained by our Umat compares well with the one obtained by the ABAQUS/STD. The same remark applies to the variation of the three components of the back stress tensor (kinematic hardening) as shown in Figure 5. The careful examination of Table 3 shows that the consistent tangent operator proposed in this study gives the same numerical performance as the ABAQUS/STD one. Note that, in Table 3, the change between the first and the second load steps corresponds to the rotation of the outward normal to the actual yield surface. In that point the proposed Umat needs one additional iteration compared to ABAQUS/SDT (see the highlighted cells in Table 3). These results show that the proposed stress computation procedure based on a consistent tangent operator possess a good numerical properties compared to the similar model available in ABAQUS/STD.

### 5.3. *Fracture prediction during hydraulic deep drawing*

The last example concerns the hydraulic deep drawing of a spherical box. Starting from a circular thin sheet ( 3.0 mm Thickness and 245.0 mm radius) fixed along its boundary on a table containing a circular hole (77.0 mm diameter), an increasing hydrostatic pressure is applied on the top of the system table/sheet giving rise to a vertical displacement of the table (2 mm/s) aiming to maintain the sheet to a fixed hemispherical punch of 72.25 mm of radius (Figure 7a). At the initial configuration the circular sheet is tangent to the top of the hemispherical punch as shown by Figure 7a. The Aluminum alloy sheet is characterized by the following material parameters : E = 84.0 GPa, $\nu$ = 0.3, $\sigma_y$ = 120.0 MPa, Q = 600.0 MPa, b = 3.0 (kinematic hardening being neglected), S = 200.0 MPa, s = $\beta$ = 1.0. The Figure 6 shows the material response of the used Aluminum in both coupled and uncoupled cases. The contact and friction between the sheet and the table is supposed of Coulomb type with friction coefficient of 0.3. Numerical simulation aims to predict where and when damaged zones can be initiated inside the formed sheet during the process.

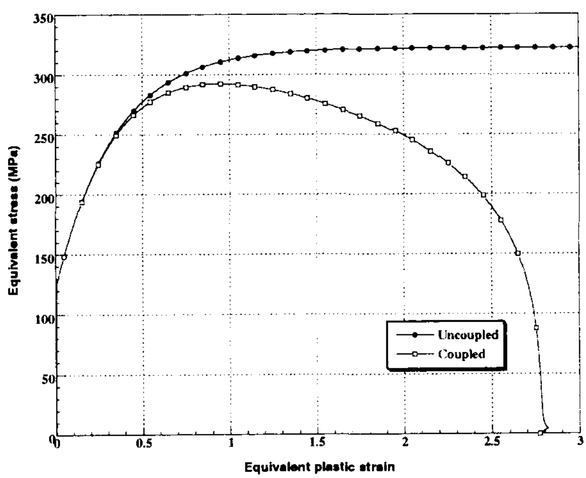


**Figure 6.** *Local response of the used material in both uncoupled and coupled cases*

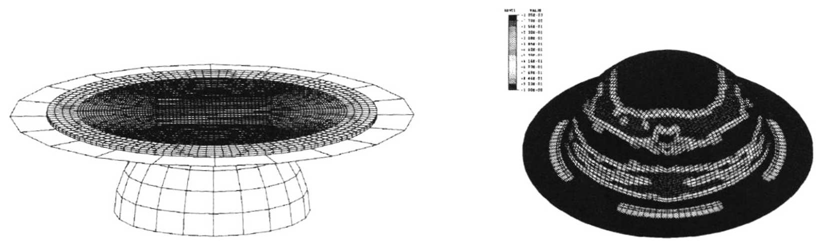

(a) Initial configuration (punch, sheet) (b) end of the process (uncoupled)

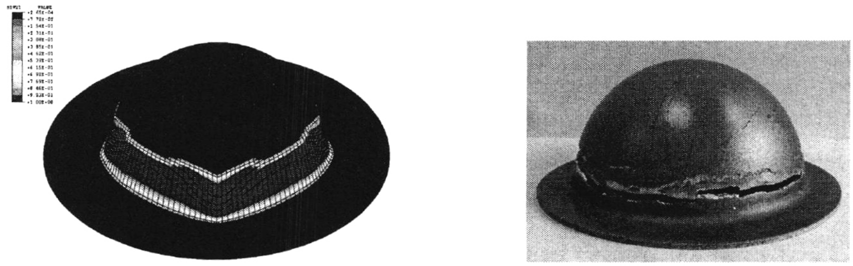

(c) end of the process (coupled) (d) end of the process (experimental)

**Figure 7.** *Damaged zones prediction during a hydraulic deep drawing process*

Figure 7 shows the comparison between the predicted (Figures 7 b,c) and the experimentally observed (Figure 7d) damaged zones at the end of the process. Figure 7b gives the numerically predicted damaged zones with the uncoupled formulation (*i.e.* no coupling between the damage and the elastoplastic behavior); while Figure 7c gives the same numerical result obtained with the fully coupled formulation. From these figures one can note that only the coupled formulation gives a result close to the experimentally observed one concerning the fully damaged zones at the end of the process. As expected, the uncoupled formulation is unable to predict correctly the location of the fully damaged zones. This shows the capability of the proposed coupled approach to predict the damage initiation location (in space and time) during metal forming processes. Many other results are available in [HAM 00].

## 6. Conclusion

The main purpose of this paper is to derive a fully implicit stress algorithm and the associated consistent tangent operator for a finite elastoplastic constitutive equations accounting for nonlinear isotropic/kinematic hardening and ductile isotropic damage. A problem-optimized procedure, which reduces the fully nonlinear system to only two scalar equations (three equations for the plane stress hypothesis) has been proposed. It has been shown that using an asymptotic integration procedure, in conjunction with the backward Euler method, leads to very good accuracy. The results obtained in the prediction of damaged zones for a 3D hydroforming process have shown the capacity of this coupled approach to optimize metal forming processes with respect to damage initiation.

It's worth noting that because the present formulation is local, the results of coupled calculations are mesh dependent. A generalization of the present model to a damage gradient formulation is under progress and will be published later.

## 7. References

[ARA 86] ARAVAS N., « The Analysis of Void Growth that Leads to Central Burst During Extrusion », *J. Mech. Phys. Solids*, 34, p. 55-79, 1986.

[BON 91] BONTCHEVA N. and IANKOV R., « Numerical Investigation of the Damage Process in Metal Forming », *Eng. Frac. Mech.*, 40, p. 387-393, 1991.

[BRU 96] BRUNET M., SABOURIN F. and MGUIL-TOUCHAL S., « The prediction of Necking and Failure in 3D Sheet Forming Analysis Using Damage Variable », *Journal de Physique III*, 6, p. 473-482, 1996.

[CHA 78] CHABOCHE, J.L., Description Thermodynamique et Phénoménologique de la viscoplasticité cyclique avec endommagement, Thèse de doctorat, Univ. Paris VI, 1978.

[CHA 96] CHABOCHE J.L. et GAILLETAUD G., "Integration methods for complex plastic constitutive equations", *Comput. Methods Appl. Mech. Eng.*, 133, p. 125-155, 1996.

[DOG 89] DOGUI, A., Plasticité anisotrope en grandes déformations, Thèse de doctorat ès-sciences, Université de Claude Bernard, Lyon 1, 1989.

[DOG 93] DOGHRI I., "Fully implicit integration and consistent tangent modulus in elasto-plasticity", *Int. J. Numer. Methods Eng.*, 36 , p. 3915-3932, 1993.

[FRE 86] FREED A.D., WLKER K.P., "Exponential integration algorithm applied to viscoplasticity", NASA TM 104461, *3rd Int. Conf. On Comput Plasticity*, Barcelona, 1992.

[GEL 85] GELIN J.C., OUDIN J. and RAVALARD Y., « An Imposed Finite Element Method for the Analysis of Damage and Ductile Fracture in Cold Metal Forming Processes », *Annals of the CIRP*, 34(1), p. 209-213, 1985.

[HAL 75] HALPHEN B., NGUYEN Q. S., "Sur les matériaux standards généralisés", *Journal de Mécanique*, 14 (39), 1975.

[HAM 00] HAMMI Y., Simulation numérique de l'endommagement dans les procédés de mise en forme, Thèse de doctorat, Université de Technologie de Troyes, Avril 2000.

[HAR 93] HARTMANN S., HAUPT P., "Stress computation and consistent tangent operator using nonlinear kinematic hardening models", *Int. J. Numer. Methods. Eng.*, 36, p. 3801-3814, 1993.

[LEM 85] LEMAITRE J. and CHABOCHE J.L., *Mécanique des Milieux Solides*, Dunod, Paris, French edition 1985, Cambridge Univ. Press, English edition, 1990.

[LEM 92] LEMAITRE J., *A course on Damage Mechanics*, Springer Verlag, 1992.

[MAT 87] MATHUR K. and DAWSON P., *Damage Evolution Modeling in Bulk Forming Processes, Computational Methods for Predicting Material Processing Defects*, Edt; Predeleanu, Elsevier, 1987.

[NAG 82] NAGTEGAAL J. C., "On the implementation of inelastic constitutive equations with special reference to large deformation problems", *Comput. Methods Appl. Mech. Eng.*, 33 (1982), p. 494-484.

[ONA 88] ONATE E. and KLEIBER M., « Plastic and Viscoplastic Flow of Void Containing Metal - Applications to Axisymmetric Sheet Forming Problem », *Int. J. Num. Meth. In Engng*. 25, p. 237-251, 1988.

[SAA 94] SAANOUNI K., FORSTER C. and BEN HATIRA F., « On the Anelastic Flow with Damage », *Int. J. Dam. Mech.*, 3, p. 140-169, 1994.

[SAA 99] SAANOUNI K. and FRANQUEVILLE Y., « Numerical Prediction of Damage During Metal Forming Processes », *Numisheet 99*, Besançon, September, France, p. 13-17, 1999.

[SAA 00] SAANOUNI K., NESNAS K. and HAMMI Y., « Damage modelling in metal forming processes », *Int. J. of Damage Mechanics*, Vol 9, n° 3, p. 196-240, July 2000.

[SAA 00] SAANOUNI K., HAMMI Y., « Numerical simulation of damage in metal forming processes », in *Continuous Damage and Fracture*, Editor A. Benallal, Elsevier, p. 353-363, 2000.

[SIM 85] SIMO J.C., TAYLOR R., "Consistent tangent operators for rate independent elastoplasticity", *Comput. Methods Appl. Mech. Eng.*, 48 (1985), p. 101-118.

[ZHU 92] ZHU Y.Y., CESCOTTO S. and HABRAKEN A.M., « A Fully Coupled Elastoplastic Damage Modeling and Fracture Criteria in Metal forming Processes », *J. Met. Proc. Tech.*, 32, p. 197-204, 1992.